Efficient Culling Techniques for Interactive Deformable NURBS Surfaces on GPU

Raquel Concheiro[1], Margarita Amor[1], Emilio J. Padrón[1] and Michael Doggett[2]
[1]*Computer Architecture Group, Universidade da Coruña, A Coruña, Spain*
[2]*Lund University Graphics Group, Lund University, Lund, Sweden*

Keywords: NURBS, Real-time and Interactive Methods, Culling Techniques, Deformable Surfaces.

Abstract: NURBS (*Non-uniform rational B-splines*) surfaces are the standard freeform representation in Computer-Aided Design (CAD) applications. Rendering NURBS surfaces accurately while they are interactively manipulated and deformed is a challenging task. In order to achieve it, the elimination from pipeline in early stages of back-facing surfaces or surface pieces is a key advantage. Furthermore, an effective interactive manipulation implies that all the culling computations should be performed for each frame, facing the possibility of fast changes in occlusion information. In this paper, different interactive culling strategies for NURBS surfaces are presented and analyzed. These culling techniques are based on the exploitation of the geometric properties presented in a NURBS surface, that allow easily to find bounds for it in screen space for each frame. Furthermore, the culling overhead for our proposals is small compared to the computational saving, outperforming a proposal without culling. An implementation of these strategies using current GPUs is presented, achieving real-time and interactive rendering rates of complex parametric models.

1 INTRODUCTION

NURBS (*Non-uniform rational B-splines*) surfaces (Piegl and Tiller, 1997) are widely employed in CAD/CAM tools and graphics applications since their essential features and qualities makes them an optimal solution for modeling complex geometries. Even though modern GPUs have introduced dedicated hardware tessellation units (Schäfer et al., 2014), these units do not always guarantee to have enough tessellation level or flexibility to render a NURBS surface with no artifacts, such as cracks, holes or creases. Furthermore, NURBS surfaces introduce considerable advantages to the on-the-fly shape manipulation of highly detailed geometry, as only a few patch control points (Smith and Schaefer, 2015) need to be handled (see Figure 1). Clearly, adaptive rendering methods to avoid the rendering of hidden surfaces or pieces of surfaces are key for performance. Thus, implementing effective and efficient culling techniques in the rendering pipeline is definitely important.

Traditionally, there have been two main approaches to render NURBS surfaces on GPU. The first alternative is based on the conversion on CPU of NURBS surfaces to other representations, such as Catmull-Clark subdivision surfaces (Shen et al., 2014) or Bézier patches (Cohen et al., 1980), that can be efficiently rendered on GPU (Guthe et al., 2005; Concheiro et al., 2010; Yeo et al., 2012; Claux et al.,

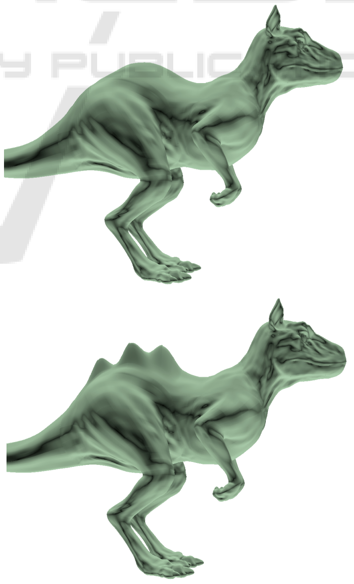
Figure 1: Shape manipulation of a NURBS surface (Killeroo Model) by interactively moving a few control points.

2014; Nießner et al., 2012). The main disadvantage of these proposals is that they can not handle deforming NURBS surfaces interactively, since costly NURBS surface to other representation conversions should be performed multiple times per frame as the surface is being deformed.

The other approach is based on rendering the NURBS surfaces directly on GPU, with no previous conversion (Krishnamurthy et al., 2007; Krishnamurthy et al., 2009; Concheiro et al., 2014). In (Krishnamurthy et al., 2007) and (Krishnamurthy et al., 2009), a previous tessellation is performed on the CPU, that creates a set of grids indicating the surface evaluation points for different levels of detail, and these data are sent to the GPU and stored as textures. In (Concheiro et al., 2014), a solution for the direct rendering of NURBS surfaces on the GPU without any previous decomposition or tessellation to Bézier surfaces is presented. This proposal, called RPNS (Rendering Pipeline for NURBS Surfaces) is based on a primitive, *KSQuad*, which uses a regular and flexible processing of NURBS surfaces, while maintaining their main geometric properties to achieve real-time rendering.

Culling is the process of removing those portions of the scene that do not contribute to the final rendering. The advantage of culling in the early stages of the rendering pipeline is that entire objects that are invisible can be removed, saving a great deal of computation in the rest of the pipeline. When dealing with polygons, one of the most traditional and standard culling techniques is Backface culling (Akenine-Möller et al., 2008), based on removing those polygons which are invisible from the viewpoint as early as possible.

Backpatch culling (Kumar et al., 1996) is an extension of backface culling to parametric surfaces, based on removing these invisible patches as early as possible. Although backpatch culling is not a novel idea, up to now it has only been applied to Bézier patches. There are basically two different groups of proposals to compute backpatch culling: based on the popular cone-of-normals approach (Munkberg et al., 2010; Sederberg and Meyers, 1988; Shirman and Abi-Ezzi, 1993) and based on the use of bounding boxes (Kumar et al., 1996; Loop et al., 2011). In the first group, (Sederberg and Meyers, 1988) proposes a cone-of-normals derived from tangent and bitangent patches, whose main drawback is the coarse bounds that are obtained. (Shirman and Abi-Ezzi, 1993) presents a preprocessing step to compute a normal patch for a given Bézier patch and to compute its bounding cone-of-normals. Next, a simple test is used to compute the culling on the fly. The main drawback of this approach is that dynamic models are not rendered in real time owing to the high computational cost. (Munkberg et al., 2010) is focused on fitting this algorithm into modern GPUs, which in turn means an approximation in the computation of the tangent and bi-tangent cone. With respect to the proposal based on the computation of the bounding box of the patches, (Kumar et al., 1996) computes the bounding box of the normalized vectors of the normal patch, whereas (Loop et al., 2011) constructs the Bézier convex hull of the parametric tangent plane. Instead of following a backpatch culling approach, in (Nießner and Loop, 2012) an occlusion culling of patches is considered.

In contrast to previous alternatives, we present an alternative solution for culling in the context of real-time NURBS rendering with the RPNS proposal. Our approach is based on the use of the *KSQuad* primitive, and takes advantage of its strong convex hull property. This makes it possible to support real-time animated and deformed models and do not require any pre-computed scene data structure. Furthermore, as shown in the next sections, this culling attains an important reduction in the number of Fragment Shader computations performed in a DirectX 11 implementation, which has a high impact on the overall performance.

The basic concepts that support our culling proposal and a brief description of RPNS are presented in Section 2.

2 RENDERING PIPELINE FOR NURBS SURFACES

The objective of RPNS is the efficient and accurate rendering of NURBS surfaces, preventing artifacts in the final image such as cracks and holes, either inside each surface or between neighbor surfaces. This makes it possible to exploit the parallelism of the GPU to perform common operations such as sketching on surfaces, interactive trimming or surface-surface intersection. Figure 2 is a block diagram of the RPNS pipeline. It consists of three shaders: Geometry, Sampler and Rasterizer.

The input stream of the Geometry shader is a primitive, denoted as KSQuad, that is based on the regions defined by the projection on the parametric cell delimited by the different knot spans. This primitive provides an efficient and accurate evaluation of NURBS surfaces in RPNS (processed in the Geometry stage, as shown in Figure 2). KSQuad needs no pre-processing stage and intrinsically maintains the main geometric properties of NURBS surfaces, such as local support and strong convex hull. The exploita-

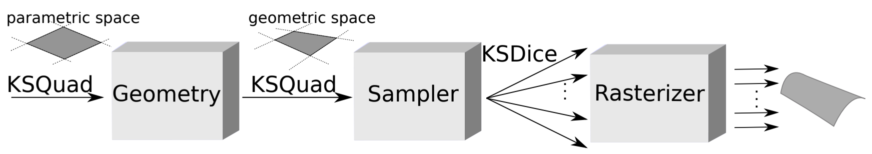

Figure 2: Basic structure of RPNS's pipeline.

tion of these properties enables us to improve performance by applying acceleration algorithms, such as the culling techniques described in Section 3.

In the Sampler shader, an adaptive sampling of the KSQuad primitives is performed according to the viewpoint, the geometric characteristics of the surface and the boundary edges between surfaces. This sampling process results in a set of sampled points or dice, denoted as KSDice and which make it possible to render the surface without cracks or holes. Each KSDie consists of a sampled point and additional information such as the parametric size of the die and the degree of the corresponding surface, and it does not save any explicit connectivity information. Think in KSDices as an artifact analogous to the idea of surfels in the context of point rendering (Pfister et al., 2000). The KSQuad discretization makes it possible to find an optimal rendering of the geometry of surfaces with minimum redundancy. Thus, a suitable discretization is obtained when it can be guaranteed that there is at least one KSDice projected into the region of each output pixel for orthographic projection. Therefore, the objective is to reduce the number of positions to be evaluated for each KSQuad primitive while keeping the quality of the resulting image.

A NURBS surface is obtained as the tensor product of two NURBS curves, parametric curves that are defined by its degree, a set of weighted control points, and a knot vector. Thus, using two independent parameters u and v, the NURBS surface of degree (p,q), respectively in both parametric directions, is given by the equation:

$$S(u,v) = \frac{\sum_{i=0}^{n}\sum_{j=0}^{m} N_{i,p}(u)\, N_{j,q}(v)\, w_{i,j}B_{i,j}}{\sum_{i=0}^{n}\sum_{j=0}^{m} N_{i,p}(u)\, N_{j,q}(v)\, w_{i,j}}, \quad 0 \le u,v \le 1$$

where $B_{i,j}$ are the control points, $w_{i,j}$ are the weights, $n+1$ and $m+1$ are the number of control points in u and v parametric directions, respectively, and $N_{i,p}$ and $N_{j,q}$ are the nonrational B-spline basis function defined on two knot vectors of $r = p+n+1$ and $s = q+m+1$ elements, respectively:

$$U = \left[\underbrace{0,\cdots,0}_{p+1}, x_{p+1},\cdots,x_{r-p-1}, \underbrace{1,\cdots 1}_{p+1} \right]$$

$$V = \left[\underbrace{0,\cdots,0}_{q+1}, y_{q+1},\cdots,y_{s-q-1}, \underbrace{1,\cdots 1}_{q+1} \right]$$

The basis function $N_{i,p}$ of degree p is defined for the parametric direction u as

$$N_{i,p}(u) = \frac{u-x_i}{x_{i+p}-x_i} N_{i,p-1}(u) + \frac{x_{i+p+1}-u}{x_{i+p+1}-x_{i+1}} N_{i+1,p-1}(u) \tag{1}$$

with

$$N_{i,0}(u) = \begin{cases} 1 & \text{if} \quad x_i \le u < x_{i+1} \\ 0 & \text{otherwise} \end{cases}$$

Analogously, the basis function $N_{j,p}$ of degree q is defined for the parametric direction v.

A NURBS surface can be seen as a grid of cells in parametric space delimited by the different knot spans, with each cell containing a part of the surface computed with the non-zero basis functions in that interval. Knot Span Quad (KSQuad), represents a half-open interval of the parametric domain, $[x_i, x_{i+1}) \times [y_j, y_{j+1})$, with non-zero length, and maintains the information of $q \times p$ neighboring knot spans, allowing an efficient evaluation of the NURBS surface in this interval. So, a KSQuad$_{i,j}$ of degree q and p is defined like

$$\text{KSQuad}_{i,j} = \{ \overbrace{x_i, x_{i+1}, y_j, y_{j+1}}^{\text{knot span}}, \underbrace{B_{i-p,j-q},\cdots,B_{i,j}}_{\text{control points}}, \overbrace{w_{i-p,j-q},\cdots,w_{i,j}}^{\text{weights}} \}$$

being $x_i \ne x_{i+1}$ and $y_j \ne y_{j+1}$.

Each KSQuad$_{i,j}$ controls a subset of the parametric domain, defined by the rectangle parametric sub-domain with corners $(x_k, y_l), k \in \{i, i+1\}, l \in \{j, j+1\}$, as illustrated in Figure 3. This sub-domain is sampled into KSDice (samples) that provide a quality render with no holes, yet increasing the performance. Pixel accurate rendering (Yeo et al., 2012), in RPNS proposal is determined by the level of samples for a

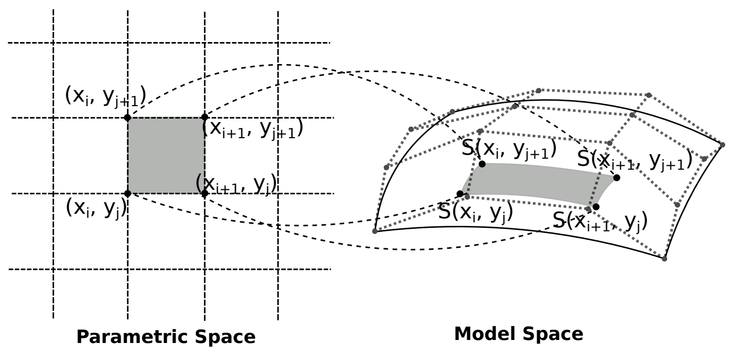

Figure 3: KSQuad primitive defined by a knot interval.

given KSQuad. In screen-spacel pixel coordinates, the samples guarantees a KSDie, by at most μ pixels:

$$\begin{aligned} \mathrm{dist}(p(S(x_k, y_k)) - p(S(x_{k+1}, y_{k+1}))) < \mu, \\ (x_i, y_j) \leq (x_k, y_k) < (x_{i+1}, y_{j+1}) \\ (x_i, y_j) < (x_{k+1}, y_{k+1}) \leq (x_{i+1}, y_{j+1}) \end{aligned} \quad (2)$$

where $p()$ means a screen space projection. For instance, $\mu = 1$ implies by at most half a pixel.

3 CULLING TECHNIQUES

One beneficial side effect of bringing forward the geometry stage prior to the sampling is that we can improve the performance by also moving forward the application of other techniques in the pipeline, such as culling. Whereas backface culling is usually performed after a tessellation step, we follow recent proposals (Hasselgren et al., 2009) which cull before tessellation to reduce as soon as possible the number of primitives to be processed. We have called BackPatch culling to this strategy, based on the original backpatch idea for Bézier from (Kumar et al., 1996), but now applied to NURBS by means of the KSQUAD artifact. Two different early culling proposals based on that idea are introduced in RPNS, performing culling before the discretization stage.

A culling algorithm generates what is called the *potentially visible set* (PVS), which is a prediction or estimation of the *exact visible set* (EVS) (Akenine-Möller et al., 2008). A PVS is conservative if it fully includes the EVS, so that only invisible geometry is discarded. Otherwise, a PVS is approximate when the EVS is not fully included, which results in rendered images with a certain error.

Our BackPatch culling strategy sends down a PVS to the next stages in the pipeline, an approximate set in one proposal and a conservative one in the other. These solutions are compared to a more classic sample-based culling solution, that generates an EVS and we have named BackDice culling, earlier presented in (Concheiro et al., 2014).

These three culling proposals are based on different approaches and placed in different pipeline stages in RPNS. BackDice culling is carried out at the end of the RPNS sampler stage (see Figure 2), once the samples have already been obtained. On the other hand, BackPatch culling must be placed at the beginning of the geometry stage, the first step in RPNS' pipeline (see Figure 2). Therefore, BackDice culling works at sample level (KSDice in RPNS), whereas the two BackPatch culling proposal do at patch level (KSQuad in RPNS).

In any case, a previous view frustum culling is applied using the NURBS' bounding box at KSQuad level. This culling, based on the strong convex hull property removes all KSQuads placed outside of the viewing cone from being considered in the following stages.

The strong convex hull property means a NURBS surface is contained in the convex hull of its control points. Moreover, if (u, v) is in the parametric rectangle defined by the knot spans $[x_i, x_{i+1}) \times [y_j, y_{j+1})$, then $S(u, v)$ is in the convex hull defined by the control points $\{B_{i-p,j-q}, \ldots, B_{i,j}\}$.

3.1 BackDice Culling

BackDice Culling (DC) is the backface culling proposal we have implemented in RPNS. It is based on the render primitive sampled from a KSQuad: KSDice. As traditional pipelines are triangle oriented in the rendering stages, culling is usually computed on triangle polygons. However, as RPNS is based on the rendering of pieces of parametric surfaces, specifically KSDice, the DiceCulling proposal removes those KSDice not turned to the camera as early as possible.

The BackDice Culling test is placed at the end of the sampler stage, after the screen-mapping procedure (see Figure 2). BackDice Culling decreases the number of KSDice sent to the rasterizer, since backfaced KSDice are culled out. However, as backface culling computations are done in the sampler stage, in this stage workload is slightly increased meanwhile the rasterizer workload is reduced.

3.2 BackPatch Culling

By applying a culling technique in the first stages of the pipeline, the number of primitives to be processed is dramatically reduced (Hasselgren et al., 2009). To prove this, two culling algorithms that exploit the versatility and flexibility offered by the use of KSQuad in the geometry stage have been implemented. These culling proposals are based on the strong convex hull property of the NURBS surfaces that is preserved in the KSQuad primitive, and it efficiently avoids the evaluation of points of knot spans which do not contribute to the final image.

Therefore, the goal of our culling proposals is to maintain the effectiveness of a conservative solution with much less computation, discarding KSQuads as early as possible in the rendering pipeline to improve overall performance for deformable surfaces. Figure 4 shows four frames of an example NURBS surface deformation. In the example, some KSQuads are fully occluded in the initial frame but visible in the following ones. As the results depicted in Section 5 prove, our culling proposal outperforms other alternatives without introducing any extra data structure, achieving an effective and efficient interactive experience when an important deformation is applied to high-detailed NURBS surfaces.

Unlike Dice Culling, designed to remove KSDice, the two backpatch culling proposals for RPNS, Lightweight BackPatch Culling (LQC) and Strong BackPatch Culling (SQC), have been designed to cull out KSQuads earlier in the pipeline. Both BackPatch Culling methods are based on the potentially visible set (PVS) and independently applied to each KSQuad, so different KSQuads of a NURBS can be culled out, whereas other ones are rendered. Consequently, KSQuads are culled before being evaluated into KSDice. This means higher computation costs in RPNS' geometry stage, but reduces the workload in the sampler and rasterizer stages.

As both techniques have been specifically designed for NURBS surfaces, they are based on the strong convex hull property previously described. Hence, the normal to the plane defined by the skeleton computed for each KSQuad is used instead of computing the normal to the KSQuad, dramatically reducing the culling computational workload.

The proposed Light Quad Culling algorithm culls a KSQuad$_{i,j}$ by using this simple square:

$$\square_{i,j} = \{S(x_i, y_j),\ S(x_{i+1}, y_j),\ S(x_i, y_{j+1}),\ S(x_{i+1}, y_{j+1})\} \tag{3}$$

LQC is an approximate PVS technique and although a fast and efficient culling computation is provided, the EVS is not fully included thus the quality of the render is slightly decreased as will be detailed in Section 5. $\square_{i,j}$ cannot guarantee that the normal of all surface points have the same direction.

On the other hand, the SQC algorithm culls a KSQuad$_{i,j}$ by computing the culling for a set of $p \times q$ squares

$$\begin{aligned}\square_{i,j}^{k,l} = \{&B_{i-p+k,j-q+l},\ B_{i-p+k+1,j-q+l},\\ &B_{i-p+k,j-q+l+1},\ B_{i-p+k+1,j-q+l+1}\}\end{aligned} \tag{4}$$

with $0 \le k \le p-1$ and $0 \le l \le q-1$. Each square is the convex hull polygon corresponding to the adjacent control points. If any of these squares is not culled, then the KSQuad is not culled. A KSQuad$_{i,j}$ is contained in the convex hull defined by the control points $\{B_{i-p,j-q}, \cdots, B_{i,j}\}$. That is, the NURBS surface fragment that defines the parametric subset KSQuad$_{i,j}$ is contained by the control net fragment, $p \times q$ squares. If any square is oriented to the viewpoint, then it is possible that any point in the surface is frontfaced. The control polygon represents a piecewise bilinear approximation to the surface. This approximation is improved by applying either knot insertion or degree elevation. As a general rule, the lower the degree, the closer the surface follows its control polygon, reaching the extreme case with $p = 1$, when the surface is the control polygon. SQC is a conservative PVS technique where the EVS is fully included, as only invisible geometries are discarded, and a high quality images are rendered.

Figure 5 shows two different scenarios for applying our culling strategies: for a high-degree surface (Figure 5a), there are few knots in the NURBS and the difference between the results obtained by the approximative and the conservative strategies, $\square_{i,j}$ and $\square_{i,j}^{k,l}$, is greater; however, for a low-degree surface (Figure 5b) the squares $\square_{i,j}$ comes close to the actual surface, so a similar PVS is obtained in both strategies, although with an marked reduction in performance in the approximative method (as shown in Section 5).

The introduction of these Quad Culling techniques in RPNS results in an important reduction in the computational load of the sampler and rasterizer stages, although this is accompanied by a slight increase in the computation of the geometry stage.

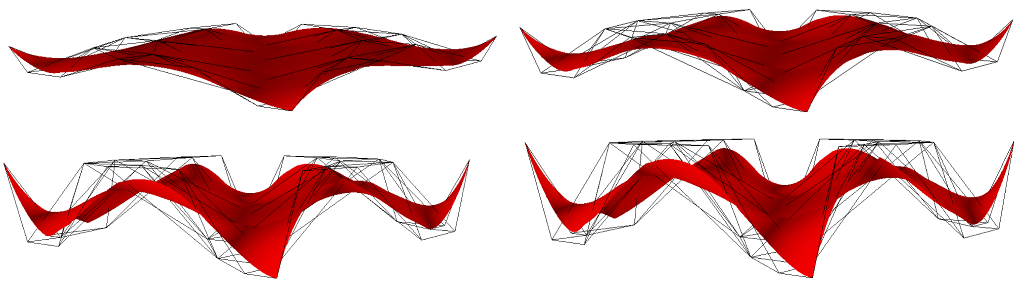

Figure 4: Example of NURBS surface deformation.

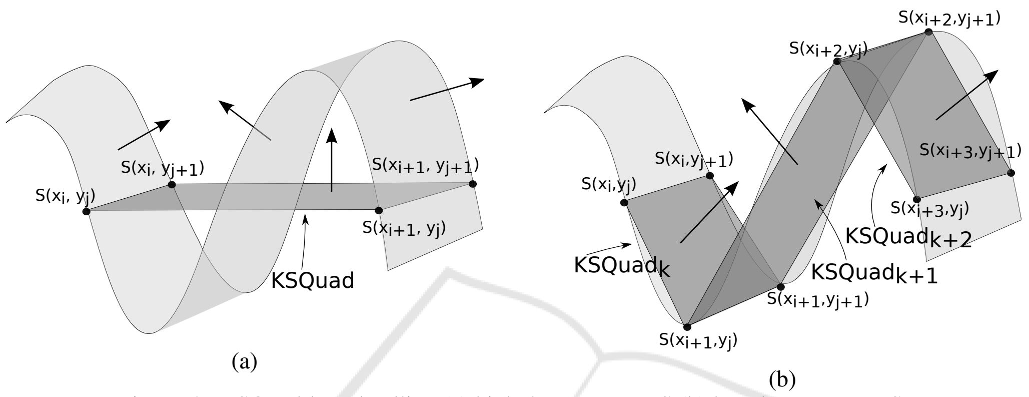

Figure 5: KSQuad-based culling (a) high degree NURBS (b) low degree NURBS.

4 TECHNIQUES OF CULLING ON CURRENT GPUS USING DIRECTX11

With DirectX11 three new stages (hull shader, tessellator unit and domain shader) were introduced to support programmable tessellation (Schäfer et al., 2014). These stages are inserted between the vertex and the geometry shader. The hull shader and the domain shader are programmable stages, whereas the unit where the real data expansion happens, the tessellator, is a configurable stage. Figure 6 depicts how a KSQuad is processed in DirectX11 according to RPNS proposal.

Hull shader is invocated once for each input primitive, KSQuad in our proposal. It is the first stage of the tessellation procedure and it configures tessellator and domain shader execution. Hence, hull shader generates two different outputs to guide the tessellation procedure, one output is sent to the domain shader while the other one is sent to the tessellator. Both outputs include the tessellation factors which are generated on-the-fly in the hull shader. In this shader a view frustum culling is applied for each KSQuad. Furthermore, LQC or SQC could be chosen to cull out KSQuad earlier in the pipeline.

Domain shader receives the parametric coordi-

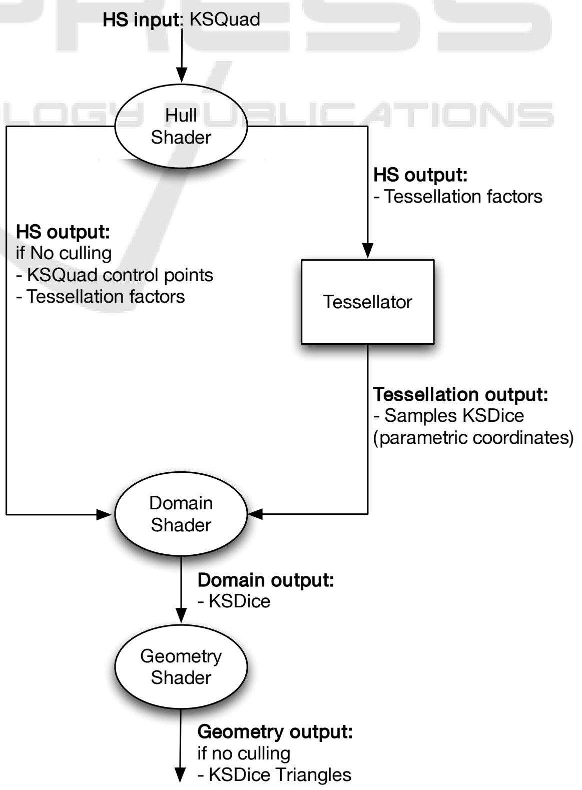

Figure 6: KSQuad processing in RPNS on DirectX11.

nates from the tessellator as well as the input primitive and the tessellator factors from the hull shader. According to the received data, these parametric coordinates are evaluated in the domain shader, that is invocated once for each parametric coordinate generated in the tessellator. The four corners of each KSDie, $S(x_k, y_l)$, $S(x_k+\delta_x, y_l)$, $S(x_k, y_l+\delta_y)$, and $S(x_k+\delta_x, y_l+\delta_y)$, are efficiently evaluated in the DS by taking advantage of access locality and avoiding redundant computations. Let us emphasize that like Reyes vertex shading, RPNS also allows the user to specify an arbitrary shading rate. In Reyes, shading rate is expressed in samples per pixel meanwhile we specify samples per KSDie in RPNS, with a value of 4.0 in our implementation. A more efficient RPNS implementation would adaptively choose the shading rate per KSDie, but that objective is beyond the scope of this paper.

The output from the DS is sent to the Geometry Shader, where two triangles are generated for each KSDie due to the triangle-oriented graphics pipeline of current GPUs. Furthermore, to optimize the rendering of NURBS surfaces we include the evaluation of EVS in the Geometry shader. This culling stage has a high impact on the overall performance, since it achieves an important reduction in the number of KSDice to get rasterized. On the other hand, in the Geometry Shader, the KSDie could be sampled again in order to assure that a higher subdivision level is applied to non-flat regions. Furthermore, a boundary region test detects the regions of KSDice that are boundaries to other surfaces and applies the highest subdivision factor to prevent cracks between adjacent surfaces.

5 EXPERIMENTAL RESULTS

In this section we present the results obtained with our culling methods implemented in RPNS. Our test platform is an Intel Core 2 Duo 2.4GHz with 2GB of RAM and a NVidia Geforce 580 GTX with DirectX11, Microsoft's HLSL. The models used in our tests are shown in Figure 7 and Table 1 depicts the number of NURBS surfaces and KSQuads, $\#NS$ and $\#KS$, respectively, in the models. As shown in Table 1 a high $\#KS$ and a low $\#NS$ are desirable due to the fact that a high amount of $\#KS$ provides a high flexibility and adaptivity inside the NURBS surface meanwhile a low $\#NS$ decreases the continuity gaps, because they can only be introduced on surface edges. The final images were rendered with a screen resolution of 2048×1152 pixels.

This analysis focuses on the number of primitives

Table 1: Number of surfaces and KSQuad for each test model.

Test model	*#NS*	*#KS*
Killeroo	89	11532
Head	601	15025
Hinge	427	34891
Car	1364	63000

generated, the quality of the rendered images, as well as the frame rate achieved. The results obtained from the tests are shown in detail in Table 2, Table 3, Table 4. The experiments were carried out for the four test models for different culling strategies and with different values of the threshold μ (maximum pixel-size for each KSDice, see Equation 2).

Table 2 depicts the thousands of KSDice that are rendered, #KS, and Table 3 shows the PSNR value (Peak Signal-to-Noise Ratio in dB) for each configuration to provide performance in terms of quality. Peak Signal-to-Noise Ratio is the distortion between the maximum possible power of a signal and the power of corrupting noise that affects the fidelity of its representation. In this case, the distortion is measured with respect to the model rendered with the maximum tessellation factor $\mathrm{PSNR} = 20 \cdot \log_{10}(\mathrm{MAX}/\sqrt{\mathrm{MSE}})$. As can be observed, similar results have being obtained in all cases. Finally, the frame rate achieved, FPS, is shown in Table 4 to provide performance in terms of rendering time.

For each culling technique implemented, Table 2 shows the percentage of KSDice eliminated. The Strong Quad Culling approach culls up to 44.45% of primitives, but there are still 1.4 times more KSDice than the strictly necessary for the rendering. The Lightweight approach culls some KSDice that should be in the rendering, so the quality of the render (PSNR value) decreases slightly. Anyhow, as PSNR tables depicts, good quality results are obtained with the three culling solutions, always over 30dB and close to 40dB for all μ values, with no significant loss of quality even with the non conservative approach (LQC). Commonly accepted reference values for PSNR are between 20 and 40dB (the bigger, the better). A value higher than 30 dB usually means that a good quality result has been achieved.

Regarding the frame rate obtained by the different culling approaches for the four test models, Table 4 shows how SQC achieves the best results. Thus, for example, speedups of 2.86 and 2.37 are obtained for $\mu = 4$ by the LQC and SQC, respectively. However, as the value of μ rises, the number of KSDice generated for each KSQuad decreases (see Table 2); this means that for values lower than 300 K KSDice the high computational cost of the HS software imple-

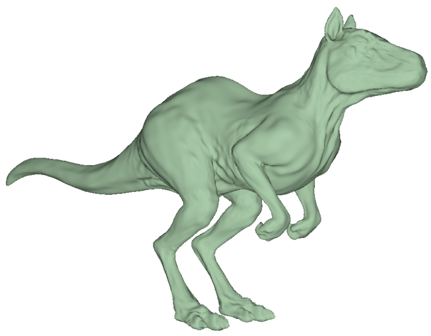
(a) *Killeroo*

(b) *Head*

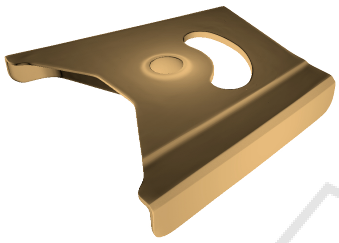
(c) *Hinge*

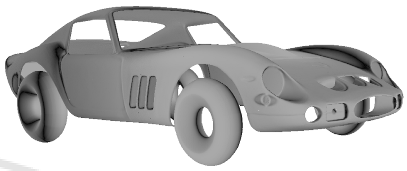
(d) *Car*

Figure 7: Test models.

Table 2: Thousands of #KS obtained with the different culling techniques for the four test models.

(a) *Killeroo*

	$\mu = 1$	$\mu = 2$	$\mu = 4$
No Culling	1564.79	485.76	178.47
DC	847.16	261.89	95.72
	54.14%	53.91%	53.63%
SQC	1564.79	378.63	139.71
	100%	77.95%	78.29%
LQC	841.98	259.90	94.82
	53.81%	53.5%	53.13%

(b) *Head*

	$\mu = 1$	$\mu = 2$	$\mu = 4$
No Culling	2309.04	742.09	225
DC	1223.83	368.87	131.85
	53%	49.71%	58.6%
SQC	1829.71	554.62	199.82
	79.24%	47.74%	88.81%
LQC	1211.38	368.28	131.23
	52.45%	49.63%	58.33%

(c) *Hinge*

	$\mu = 1$	$\mu = 2$	$\mu = 4$
No Culling	4245.46	1593.56	576.54
DC	1578.48	716.35	252.02
	62.81 %	55.04 %	56.28%
SQC	2977.54	907.97	325.36
	29.86%	43.02%	43.56%
LQC	2373.27	716.07	251.76
	44.09 %	55.06%	56.33%

(d) *Car*

	$\mu = 1$	$\mu = 2$	$\mu = 4$
No Culling	4448.50	1493.51	607.11
DC	2520.33	839.08	311.96
	56.66%	56.18%	51.38%
SQC	3444.57	1149.10	459.18
	56.81%	56.22%	55.25%
LQC	2527.32	839.68	335.44
	77.43%	76.94%	75.63%

mentation, that has a significant degree of divergence, spoils the advantage achieved by reducing the number of KSDice to be rendered in cases with similar tessellation factors for all the surfaces, so the frame rate drops. In this case, the best results are obtained by the Dice Culling implementation, since the backface KSDice are removed with very simple computations with no divergence on the GS. Otherwise, the BackPatch

Table 3: PSNR obtained with the different culling techniques for the four test models.

(a) *Killeroo*

	$\mu=1$	$\mu=2$	$\mu=4$
No Culling	44.51	42.95	40.75
DC	44.50	42.95	40.75
SQC	44.53	42.95	40.75
LQC	39.16	38.64	38.22

(b) *Head*

	$\mu=1$	$\mu=2$	$\mu=4$
No Culling	42.37	43.93	42.97
DC	42.36	43.86	42.57
SQC	42.36	43.95	42.57
LQC	38.88	38.41	38.21

(c) *Hinge*

	$\mu=1$	$\mu=2$	$\mu=4$
No Culling	41.89	41.39	39.77
DC	41.02	41.65	39.94
SQC	41.11	41.42	39.78
LQC	40.60	41.29	39.70

(d) *Car*

	$\mu=1$	$\mu=2$	$\mu=4$
No Culling	38.64	38.35	40.47
DC	38.53	38.34	40.45
SQC	38.54	38.34	40.48
LQC	34.87	34.47	35.25

Table 4: FPS obtained with the different culling techniques for the four test models (speedup against no culling is also shown).

(a) *Killeroo*

	$\mu=1$	$\mu=2$	$\mu=4$
No Culling	27.91	76.14	152.7
DC	26.43	73.1	165.21
	0.95x	0.96x	1.08x
SQC	34.46	87.51	162.78
	1.23x	1.15x	1.06x
LQC	47.44	107.12	179.9
	1.70x	1.41x	1.18x

(b) *Head*

	$\mu=1$	$\mu=2$	$\mu=4$
No Culling	17.90	41.84	113.03
DC	20.66	54.6	158.48
	1.15x	1.30x	1.40x
SQC	21.44	49.83	54.56
	1.20x	1.19x	0.48x
LQC	33.67	90.24	122.52
	1.88x	2.16x	1.08x

(c) *Hinge*

	$\mu=1$	$\mu=2$	$\mu=4$
No Culling	9.27	27.57	35.22
DC	8.55	26.21	64.94
	0.92x	0.95x	1.84x
SQC	15.35	44.49	83.42
	1.66x	1.61x	2.37x
LQC	19.01	53.73	100.65
	2.05	1.95	2.86

(d) *Car*

	$\mu=1$	$\mu=2$	$\mu=4$
No Culling	10.23	20.31	33.3
DC	9.59	29.91	59.18
	0.94x	1.47x	1.77x
SQC	12.85	34.9	58.9
	1.26x	1.72x	1.77x
LQC	17.06	44.37	70.56
	1.67x	2.18x	2.12x

Culling implementations may still be worthwhile for values between 300 K and 200 K KSDice in models such as *Killeroo*. In this model, there are KSDice with much higher tessellation factors than others as they have a greater area in the projected image. These large KSQuads are an important bottleneck, so performance dramatically improves when they are culled. Thus, 182.7 K KSDice are generated without culling with $\mu = 4$ for the *Killeroo* model, achieving 179.9 and 165.21fps with the LQC and the DC solutions, respectively. Therefore, BackPatch Culling attains the best performance results for the more complex models, those for which the profit of culling is more noticeable.

Regarding the performance attained with our implementations in the pipeline of current GPUs, Ta-

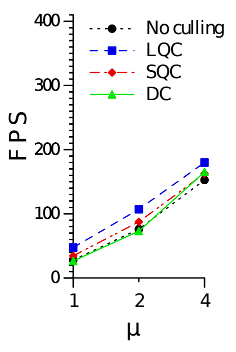

(a) *Killeroo*

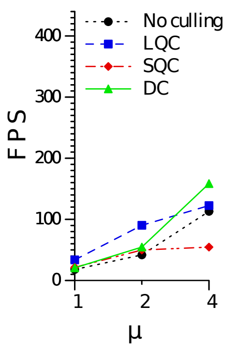

(b) *Head*

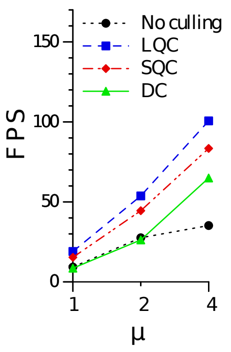

(c) *Hinge*

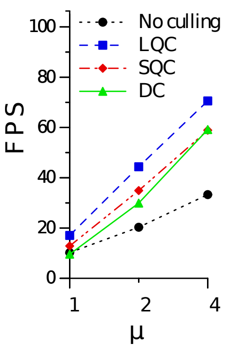

(d) *Car*

Figure 8: Frame rate with the different culling approaches for the four test models.

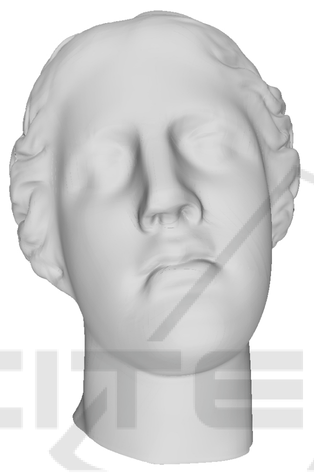

(a)

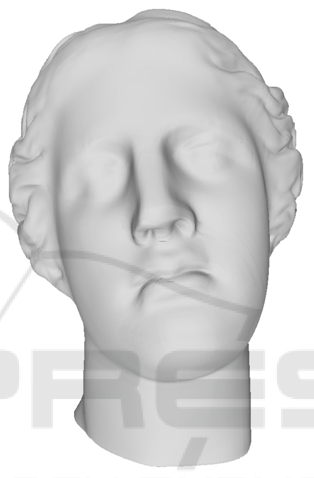

(b)

Figure 9: Model *Head* rendered (a) without any culling (b) with culling.

ble 4 shows the good results in terms of frame rate obtained with $\mu \geq 1$ for the four test models. These results are also depicted in the graphs of Figure 8. The tables and the graphs show that the introduction of BackPatch culling dramatically improves the performance of the pipeline, with speed-ups of more than 2x in the frame rate in some cases, and without decreasing the quality in the rendering, since the PSNR values are mostly identical. In these cases, the number of primitives culled in an early stage of the pipeline is not worth the additional computation introduced with these backpatch strategies such as LQC and SQC. Backpatch culling strategies are applied to KSQuad primitives in an early pipeline stage, while KSDice primitives are culled out in a latter GPU pipeline stages in a more classical backface culling approach. Consequently, backpatch culling strategies evaluate considerable fewer primitives than the backface culling strategy. In any case, the final rendering obtained by RPNS is a high quality image, as proved by the PSNR results. Two different renders of the model *Head* are shown in Figure 9, without any culling on the left and with it on the right.

To sum up, the culling techniques proposed in this work remove an average of around a 20% of the KS-Dice generated in the case of the SQC method and over a 41% when the LQC is applied. Both strategies achieve good results in terms of quality, always over 30 *dB*, as has previously been mentioned.

6 CONCLUSIONS

In this paper, we provide culling techniques to NURBS surfaces which cull earlier stage of the pipeline to reduce as soon as possible the number of primitives to be processed. Specifically, we have developed two new efficient culling techniques, Lightweight BackPatch Culling (LQC) andStrong BackPatch Culling (SQC), based on the strong convex hull property of NURBS surfaces that allows a small culling overhead compared to the computational savings, Our proposals have been implemented in DirectX11 to achieve interactive handling of NURBS surfaces. SQC achieves up to 2.37x speedup over non-culling proposal whereas LQC up to 2.86x.

As future work, our primary focus is to apply our culling proposal to handle motion blur rasterization (Gribel et al., 2013). We also plan to extend our proposal to consider self-collision detection (Wong et al., 2014).

ACKNOWLEDGEMENTS

This research has been supported by the Galician Government (Xunta de Galicia) under the Consolidation Program of Competitive Reference Groups, cofunded by FEDER funds of the EU (Ref. GRC2013/055); and by the Ministry of Economy and Competitiveness of Spain and FEDER funds of the EU (Project TIN2013-42148-P).

REFERENCES

Akenine-Möller, T., Haines, E., and Hoffman, N. (2008). *Real-Time Rendering*. A. K. Peters.

Claux, F., Barthe, L., Vanderhaeghe, D., Jessel, J.-P., and Paulin, M. (2014). Crack-free rendering of dynamically tesselated B-rep models. *Computer Graphics Forum*, 33(2):263–272.

Cohen, E., Lyche, T., and Riesenfeld, R. (1980). Discrete B-splines and subdivision techniques in computer-aided geometric design and computer graphics. *Computer Graphics and Image Processing*, 14(2):87–111.

Concheiro, R., Amor, M., and Bóo, M. (2010). Synthesis of Bézier surfaces on the GPU. In Richard, P., Braz, J., and Hilton, A., editors, *Proceedings of the GRAPP'10: International Conference on Computer Graphics Theory and Applications*, pages 110–115. INSTICC Press.

Concheiro, R., Amor, M., Padrón, E. J., and Doggett, M. C. (2014). Interactive rendering of NURBS surfaces. *Computer-Aided Design*, 56:34–44.

Gribel, C. J., Munkberg, J., Hasselgren, J., and Akenine-Möller, T. (2013). Theory and analysis of higher-order motion blur rasterization. In *Proceedings of the 5th High-Performance Graphics Conference, HPG'13*, pages 7–15.

Guthe, M., Balázs, Á., and Klein, R. (2005). GPU-based trimming and tessellation of NURBS and T-Spline surfaces. *ACM Transactions on Graphics*, 24(3).

Hasselgren, J., Munkberg, J., and Akenine-Möller, T. (2009). Automatic pre-tessellation culling. *ACM Trans. Graph.*, 28(2):19:1–19:10.

Krishnamurthy, A., Khardekar, R., and McMains, S. (2007). Direct evaluation of NURBS curves and surfaces on the GPU. In *Proceedings of SPM'07: The 2007 ACM Symposium on Solid and Physical Modeling*, pages 329–334.

Krishnamurthy, A., Khardekar, R., McMains, S., Haller, K., and Elber, G. (2009). Performing efficient NURBS modeling operation on the GPU. *IEEE Transactions on Visualization and Computer Graphics*, 15(4):530–543.

Kumar, S., Manocha, D., and Lastra, A. (1996). Interactive display of large-scale NURBS models. *IEEE Transactions on Visualization and Computer Graphics*, 2(4):323–336.

Loop, C. T., Nießner, M., and Eisenacher, C. (2011). Effective back-patch culling for hardware tessellation. In *Proceeding of the VMV 2011: Vision, Modeling, and Visualization Workshop*, pages 263–268.

Munkberg, J., Hasselgren, J., Toth, R., and Akenine-Möller, T. (2010). Efficient bounding of displaced Bézier patches. In *Proceedings of the Conference on High Performance Graphics, HPG'10*, pages 153–162. Eurographics.

Nießner, M. and Loop, C. (2012). Patch-based occlusion culling for hardware tessellation. In *Proceedings of the Computer Graphics International 2012, CGI'12*.

Nießner, M., Loop, C., Meyer, M., and DeRose, T. (2012). Feature adaptive GPU rendering of Catmull-Clark subdivision surfaces. *ACM Transactions on Graphics*, 31(1).

Pfister, H., Zwicker, M., van Baar, J., and Gross, M. (2000). Surfels: surface elements as rendering primitives. In *Proceedings of the SIGGRAPH'00: 27th annual conference on Computer graphics and interactive techniques*, pages 335–342, New York, NY, USA. ACM Press/Addison-Wesley Publishing Co.

Piegl, L. and Tiller, W. (1997). *The NURBS Book*. Springer.

Schäfer, H., Nießner, M., Keinert, B., Stamminger, M., and Loop, C. (2014). State of the art report on real-time rendering with hardware tessellation. In *Eurographics, State of the Art Reports*.

Sederberg, T. W. and Meyers, R. J. (1988). Loop detection in surface patch intersections. *Computer Aided Geometric Design*, 5(2):161–171.

Shen, J., Kosinka, J., Sabin, M. A., and Dodgson, N. A. (2014). Conversion of trimmed NURBS surfaces to CatmullClark subdivision surfaces. *Computer Aided Geometric Design*, 13(7–8):486–498.

Shirman, L. A. and Abi-Ezzi, S. S. (1993). The cone of normals technique for fast processing of curved patches. *Computer Graphics Forum*, 12(3):261–272.

Smith, J. and Schaefer, S. (2015). Selective degree elevation for multi-sided Bézier patches. *Computer Graphics Forum*, 34(2).

Wong, S.-K., Lin, W.-C., Wang, Y.-S., Hung, C.-H., and Huang, Y.-J. (2014). Dynamic radial view based culling for continuous self-collision detection. In *Proceedings of the 18th meeting of the ACM SIGGRAPH Symposium on Interactive 3D Graphics and Games, I3D'14*, pages 39–46.

Yeo, Y. I., Bin, L., and Peters, J. (2012). Efficient pixel-accurate rendering of curved surfaces. In *Proceedings of the i3D'12: ACM SIGGRAPH Symposium on Interactive 3D Graphics and Games*, pages 165–174, New York, NY, USA. ACM.